

A model for upper kHz QPO coherence of accreting neutron star

J. Wang¹, C. M. Zhang¹, Y. H. Zhao¹, Y. F. Lin,² H. X. Yin³, L. M. Song⁴

¹ National Astronomical Observatories, Chinese Academy of Sciences, Beijing 100012, P. R. China, jwang@bao.ac.cn, zhangcm@bao.ac.cn

²Department of Physics and Tsinghua Center for Astrophysics, Tsinghua University, Beijing 100084, China

³School of Space Science and Physics, Shandong University, Weihai 264209, China

⁴Institute of High Energy Physics, Chinese Academy of Sciences, Beijing 100049, China

the date of receipt and acceptance should be inserted later

Abstract. We investigate the coherence of the twin kilohertz quasi-periodic oscillations (kHz QPOs) in the low-mass X-ray binary (LMXB) theoretically. The profile of upper kHz QPO, interpreted as Keplerian frequency, is ascribed to the radial extent of the kHz QPO emission region, associated with the transitional layer at the magnetosphere-disk boundary, which corresponds to the coherence of upper kHz QPO. The theoretical model for Q-factor of upper kHz QPO is applied to the observational data of five Atoll and five Z sources, and the consistence is implied.

Key words. accretion: accretion disks–stars; neutron–binaries; close–X-rays: stars–pulsar

1. Introduction

The launch of the Rossi X-ray Timing Explorer (RXTE) led to the discovery of Kilohertz quasi-periodic oscillations (kHz QPOs) of X-ray spectra in low-mass X-ray binaries (LMXBs), i.e., narrow features in their power density spectra (PDS) (van der Klis 2000, 2006). These frequencies, in the range of 200 ~ 1300 Hz, are the same order of the dynamical time-scales of the innermost regions of the accretion flow around the stellar mass compact objects (van der Klis 2006, 2008), which may carry imprints of strong field general relativity phenomena (e.g. Kluzniak, Michelson, Wagoner 1990; Miller, Lamb & Psaltis 1998; Kluzniak 1998; Abramowicz et al. 2003). Owing to the expected links with the orbital motion, most works about the kHz QPOs focus on the explanation for the emission of these frequencies of the orbital Keplerian motion (e.g. Miller, Lamb & Psaltis 1998; Stella & Vietri 1998, 1999; Kluzniak & Abramowicz 2001; Abramowicz et al. 2003; Zhang 2004). In addition, the kHz QPOs were found to occur in twin peaks usually (upper ν_2 and lower ν_1 frequency). They behave in a rather regular way and follow the tight correlations between their frequencies and other observed characteristic frequencies (see, e.g. Psaltis et al. 1998, 1999a; Psaltis, Belloni & van der Klis 1999b; Stella, Vietri & Morsink 1999; Belloni, Psaltis & van der Klis 2002; Titarchuk & Wood 2002; Méndez & van der Klis 1999, 2000; Méndez et al. 2001; Yu W. F., van der Klis M., Jonker P. G. 2001; Yu W. F., van der Klis M. 2002). Moreover, the correlation between the upper frequency and lower frequency across different sources can be roughly fitted by a power-law function (see e.g. Psaltis et al. 1998, 1999a;

Zhang et al. 2006a), and also by a linear model (see Belloni, Méndez & Homan 2005, 2007).

The kHz QPOs in LMXB are typical time variable signals and peaks with some width in PDS, with the particular case of the sharp coherent pulsation 401 Hz and a near 401 Hz X-ray burst oscillation frequency are found in SAX J1808.4-3658 (Chakrabarty et al. 2003; Wijnands et al. 2003; Wijnands 2005), whose profiles can be described by a Lorentzian Function (see the lower panel in Fig. 1),

$$P_\nu \propto A_0 w / [(v - \nu_0)^2 + (w/2)^2], \quad (1)$$

where ν_0 is the peak frequency, w is the full width at half-maximum (FWHM), and A_0 is the amplitude of this signal. The ratio of these two quantities are the quality factor, i.e.,

$$Q \equiv \frac{\nu_0}{w}. \quad (2)$$

This function is characterized by three characteristic quantities which are used to describe the profile of these signals, i.e. centroid frequency (i.e. peak frequency ν_0), quality factor ($Q \equiv \nu_0 / \text{FWHM}$) and the fractional root-mean-squared (rms). The quality factor characterizes the coherence of a QPO signal, while the rms represents a measure of the signal strength, which is proportional to the square root of the peak power contribution to the PDS. The large RXTE archive makes possible searches for systematic correlations between these three characteristic quantities. Using data from RXTE, Barret et al. (2005a) studied 4U 1608-52 and revealed a positive correlation between lower frequency and its quality factor, up to a maximum of about $Q \sim 200$. Motivated by this idea, Barret, Olive & Miller (2005b, 2006) studied, in a systematic way, the QPO properties of 4U 1636-536 and the dependency of quality factor and

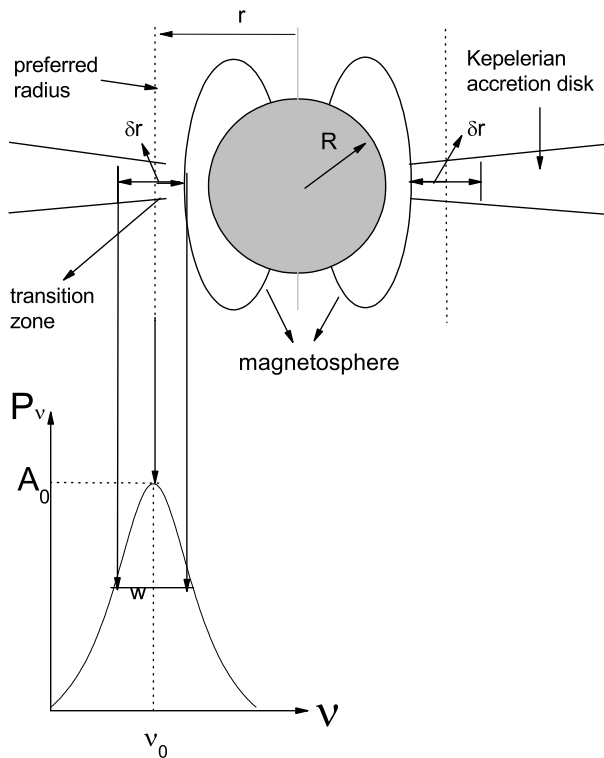


Fig. 1. The illustration of Lorentzian function as described in Eq. (1) is associated with the sketch map of the magnetosphere-disk transition layer. The labels A_0 , ν_0 and w are noted in Lorentzian function Eq.(1). In the upper panel of figure, the stellar radius R , magnetosphere radius r and magnetosphere-disk transition layer width δr are noted, and the kHz QPO profile and its corresponding positions in the transition layer are presented.

rms on frequency. It is shown that quality factors for the lower and upper kHz QPOs of 4U 1636-536 follow different tracks in a Q versus frequency plot, i.e. quality factor for the lower kHz QPO increases with frequency up to 850 Hz ($Q \sim 200$) and drops precipitously to the highest detected frequencies ~ 920 Hz ($Q \sim 50$), while that of the upper kHz QPO increases steadily all the way to the highest detectable QPO frequency. Moreover, quality factor of the lower QPO is higher than that of the upper (Barret, Olive & Miller 2005b,c; 2006). In addition, the fractional rms amplitudes of both the upper and lower kHz QPOs increase then decrease steadily towards higher frequencies, with a ceiling in lower kHz QPO (Barret, Olive & Miller 2005b,c; 2006). A similar behavior was seen from 4U 1608-52 (Barret et al. 2005a). The rough similarity also was extended to 4U 1735-44, 4U 1728-34 (Barret, Olive & Miller 2006; Boutelier, Barret & Miller 2009; Méndez 2006; Török 2009). The complete list of references on QPOs from these sources is available in van der Klis (2006). Then Török (2009) studied the difference in rms amplitude between the upper and lower kHz QPOs as a function of the frequency ratio (ν_2/ν_1). They found that the rms amplitudes of the twin peaks become equal when the frequencies of the oscillations pass through a certain ratio (ν_2/ν_1), which is roughly the same for each of

the sources. It is also predicted that in a more general context, the behaviour of the amplitude difference suggests a possible energy interchange between the upper and lower QPO modes (Török 2009).

Theoretically, the quality factor and rms amplitude have also been studied but not yet satisfactorily settled. In the past years, several works, focussing on the quality factor and rms as separated functions of frequencies, have been discussed on these properties, and possible consequences for various QPO models have been outlined (see, e.g., Barret et al. 2005a; Méndez 2006; Barret, Olive & Miller 2006, for further information and references). Méndez (2006) considered the relation between the innermost stable circular orbit (ISCO) and the drop of QPO coherence and rms. Barret, Olive & Miller (2006) discussed the implications of their results and showed how the high-frequency drop-off in quality factor can be accommodated quantitatively in a toy model based on the approach to the ISCO. In their toy model, the change of quality factor was ascribed to three basic parts: (1) the finite extent in radial direction (Δr_{orb}), (2) the radial drift (Δr_{drift}) during the lifetime of the oscillation, (3) the finite time itself (Barret, Olive & Miller 2006). It was also proposed that a drop in the amplitude and quality factor of the QPOs at some limiting frequency is a possible signature of the ISCO (Miller, Lamb & Psaltis 1998; Barret, Olive & Miller 2005b,c).

The abrupt rise of X-ray flux, as a cause of QPO, may be related to the abrupt transformation of environment in accretion process, which is ascribed to the interaction of magnetosphere dominated regime and gravitational induced energy-momentum dominated disk. In this regards, the interpretation of the twin kHz QPOs has been ascribed to the orbital Keplerian frequency at magnetosphere-disk boundary for upper kHz QPO and MHD Alfvén wave propagation frequency there for lower kHz QPO, respectively (Zhang 2004; Zhang et al. 2007). The quality factor can be attributed to the radial extent of the transition zone where kHz QPOs produce (see Fig. 1). In this letter, we investigate how this radial extent leads to the profile for upper kHz QPO, which is described in Section 2, where the comparison between theory and observations is also presented. Section 3 contains the conclusions and discussions.

2. Formation of High Q Factor and Its Variation with Frequency

According to the MHD Alfvén wave oscillation model of kHz QPO, the MHD turbulence by the shear flow in the accretion disk (e.g., Ruediger & Pipin 2000) will trigger the strong variation of plasma energy density and ignite the shear Alfvén wave motion along the orbit with the loop length of circumference $2\pi r$ at the Keplerian disk orbit radius r (Zhang et al. 2007). In the process of NS accretion, there is a transition from the spherical accretion with high mass density to a polar cap accretion with low mass density (Zhang 2004). It is assumed that this transition occurred at a certain radius which is called preferred radius, where a MHD tube loop may be formed to conduct the accreted matter to the polar cap of star. This critical transition may give rise to MHD turbulence and perturb the field lines, thus excite Alfvén wave oscillation. In such a sce-

nario, the lower and upper frequency correspond to the AWOFF with the spherical accretion mass density which coincides with the Keplerian orbital frequency ν_k and the AWOFF with the polar accretion mass density, respectively. At the preferred radius r which is defined by the magnetic pressure matching the ram pressure, these two frequencies read (Zhang 2004), respectively,

$$\nu_2 = \sqrt{\frac{GM}{4\pi^2 r^3}} = 1850(Hz)AX^{\frac{3}{2}}, \quad (3)$$

$$\nu_1 = \nu_A(S_p) = \nu_2 \sqrt{\frac{S_p}{S_r}} = \nu_2 X \sqrt{1 - \sqrt{1 - X}}. \quad (4)$$

Here, the NS mass M is in units of solar mass, and $\nu_A \propto \sqrt{S}$ is the AWOFF where the area S representing the spherical area $S_r = 4\pi R^2$ or the polar cap area $S_p = 4\pi R^2(1 - \sqrt{1 - X})$, respectively. $X = \frac{R}{r}$ is the ratio between star radius R and disk radius r . $A = (m/R_6^3)^{1/2}$ with $R_6 = R/10^6(\text{cm})$ and m the mass M in the units of solar masses.

We ascribe the upper kHz QPO frequency profile to the X-ray flux strong variations from transition layer, as shown in the upper panel of Fig.(1). Thus, the range of the upper frequency ($\delta\nu$) should be the indication of transition layer radial extent (δr or in terms of the scaled quantity X).

$$\delta\nu_2 = \nu_2 \frac{3\delta X}{2X} = \nu_2 \frac{3\delta r}{2r}. \quad (5)$$

If we set the QPO FWHM w as corresponding to the scale of transition layer width, i.e. $w \sim \delta\nu$, then the quality factor for upper frequency (hereafter upper Q-factor) can be written as,

$$Q_2 = \frac{\nu_2}{\delta\nu_2} = \frac{2}{3} \frac{r}{\delta r}. \quad (6)$$

We consider a transition layer (see upper panel of Fig. (1)) between the innermost Keplerian orbit and the magnetosphere (Elsner & Lamb 1977; Naso & Miller 2010ab), in which the transition for radial velocity of accretion flow from a Keplerian to a corotation with the NS may occur (Titarchuk, Lapidus & Muslimov 1999 hereafter TLM; Titarchuk & Osherovich 1999). But in this region the formation of kinks and shocks due to the inhomogeneous density of flow and supersonic motions of accretion flow may be responsible for a super-Keplerian rotation (TLM). After a self-adjustment which is the function of this layer, the coupling of the sub-Keplerian flow with the super-Keplerian rotation still leads to a Keplerian zone which contributes to the radial drift. When the accreted matter fall into the innermost Keplerian orbit and transition zone, these plasma may strike the magnetospheric boundary and bend the field lines, which lead to the change of the magnetospheric shape due to the strong ram pressure and can excited the Alfvén wave oscillation. In the meantime, the plasma is threaded by the field lines and fall onto the polar cap. However, on the magnetospheric boundary, the accreted matter carries different velocities and has different density from the former arrivals, which bring into some instabilities, such as Kelvin-Helmholtz instability, Rayleigh-Taylor instability, and the inhomogeneities caused by the azimuthal component of the field trapped inside the inner regions of the disk (Romanova, Kulkarni & Lovelace

2007). The Kelvin-Helmholtz instability seems to be less significant (Rastätter & Schindler 1999), and we just focus on the Rayleigh-Taylor instability (Kulkarni & Romanova 2008). The unstable disc-magnetosphere boundary results in the penetration of the magnetosphere by the disc matter in kinds of forms. In addition, the disc matter treading the field lines into the magnetosphere from polar cap may move to the equatorial region and swell the magnetosphere. On the grounds of this idea and the geometry of accretion disc boundary layer (Regev & Hougerat 1988), the radial extent direction can be written as (Elsner & Lamb 1977; Naso & Miller 2010ab),

$$\delta r = \alpha(r - R), \quad (7)$$

where the quantity $(r-R)$ stands for the scale of the magnetosphere-disk boundary to stellar surface, and $\alpha < 1$ is a constant ratio coefficient. Therefore, we can obtain,

$$Q_2 = \frac{2}{3\alpha} \left(1 - \frac{R}{r}\right)^{-1} = \frac{2}{3\alpha} (1 - X)^{-1}. \quad (8)$$

Using the definition of X and Eq. (3), we can write Q_2 with respect to the upper frequency,

$$Q_2 \sim \alpha^{-1} \left[1 - \left(\frac{\nu_2}{1850A}\right)^{\frac{2}{3}}\right]^{-1}. \quad (9)$$

For the detected twin kHz QPOs, the mass density parameter A is found to be about 0.7 (e.g. Sco X-1) (Zhang 2004; Zhang et al. 2007), except for the two unusual X-ray millisecond pulsar cases SAX J1804.5-3654 and XTE J1807-294, $A=0.45$ and 0.4 respectively (Zhang et al. 2010). In most cases (except Cir X-1), the position parameter $X=R/r$ lies in the range from 0.7 to 0.92, or the kHz QPO emission position radius is from $r=1.1R$ to $r=1.4R$ (Zhang et al. 2010). Averagely, we have the following expression to evaluate the upper Q-factor,

$$Q_2 \sim \alpha^{-1} \left[1 - \left(\frac{\nu_2}{1300(\text{Hz})}\right)^{\frac{2}{3}}\right]^{-1}. \quad (10)$$

To make a comparison between the model and the detections of the upper Q-factor, we firstly put the sources whose spectrum of kHz QPOs displayed the high coherence together in Fig. 2. **We choose the parameter $\alpha = 0.35, 0.55, 0.8$, respectively, and plot the theoretical curves. Then we fit the theoretical expression for Q_2 (Eq. (10)) to the observational data and find that the model curve with $\alpha = 0.551$ fits the most data well, i.e. the radial extent of the preferred radius is about half of the thickness of the magnetosphere-disk boundary to stellar surface (see Fig. 2). It is can be seen that five Z sources and five Atoll sources (Hasinger 1989, 1990) show different coherence trends, which are described in Fig. 3, as the same meanings of Fig. 2 but with the separate sources for a clearly presentation. The fitting results are listed in Table 1.** For the Atoll source 4U 1728-34, there is an abrupt drop at $\nu \sim 1050$ Hz in the $Q-\nu$ plot, then it is argued as an effect of innermost stable orbit (Barret, Olive & Miller 2005b,c; 2006) to arise this abrupt kHz QPO profile changes.

3. Conclusions and Discussions

We try to ascribe the profile of upper kHz QPO frequency to the radial extent of its emission region at magnetosphere-disk

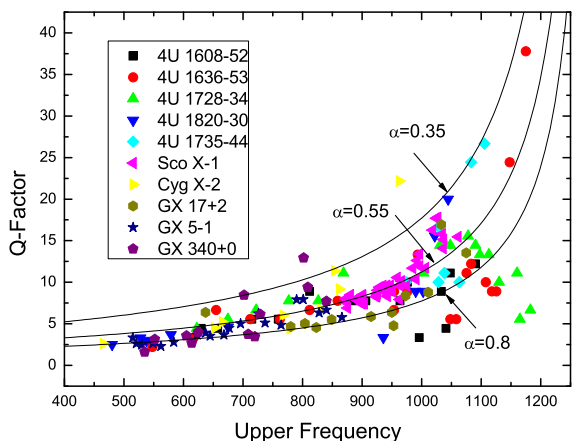


Fig. 2. Plot for the upper Q-factor versus its frequency. The data are provided by D. Barret and M. Mendez, which have been exploited and discussed in the references (Barret et al. 2005abc, 2006, 2007, 2008; Boutelier et al. 2009, 2010; Mendez 2006). The theoretical curves of upper Q-factor Q_2 of Eq. (10) are plotted with the parameter $\alpha = 0.35, 0.55, 0.8$ and the averaged mass density parameter $A=0.7$ (Zhang 2004; Zhang et al. 2007).

Table 1. The fitting results for the observation data.

Source	α	error(α)	χ^2/DoF	error(χ^2/DoF)
Total	0.551	0.030	3.729	0.601
4U 1728-34	0.400	0.033	2.007	0.452
4U 1735-44	0.400	0.027	14.095	5.337
Sco X-1	0.650	0.007	1.391	0.539
Cyg X-2	0.530	0.039	2.186	1.378
GX 17+2	0.800	0.0340	6.015	1.463
4U 1820-30	0.530	0.040	1.741	0.522
GX 340+0	0.600	0.042	6.416	2.068
GX 5-1	0.800	0.022	1.669	0.047
4U 1636-53	0.530	0.027	4.540	0.450
4U 1608-52	0.650	0.027	5.183	1.020

transition layer, and investigate the evolutions of its quality factor as a function of upper frequency. The central frequency of upper kHz QPO emits from a preferred radius r , at which the magnetic pressure matches the ram pressure of the inward disk material, and the radial extent of the preferred radius contributes to the frequency extension of the upper kHz QPOs. The narrower this extent, the higher coherence of QPO (or upper Q-factor). After making the comparisons between the model and detected Q-factor data (Fig. 2), we find that the radial extent δr accounts for about half of the transition zone, extending from the stellar surface to the magnetosphere-disk boundary, e.g. ($r-R$). This means that X-ray flux from this radial extent primarily contributes to the QPO peak profile (see illustration figure Fig.1). On the quantitatively discussion of the kHz QPO emission region, we refer to the recent result by Zhang (2010) that the kHz QPOs of most sources emit from the positions at $r \sim 20$ km if stellar radius $R=15$ km is assumed (excluding Cir X-1, its emission position is slightly far from star, e.g. $r \sim 30$ km), thus

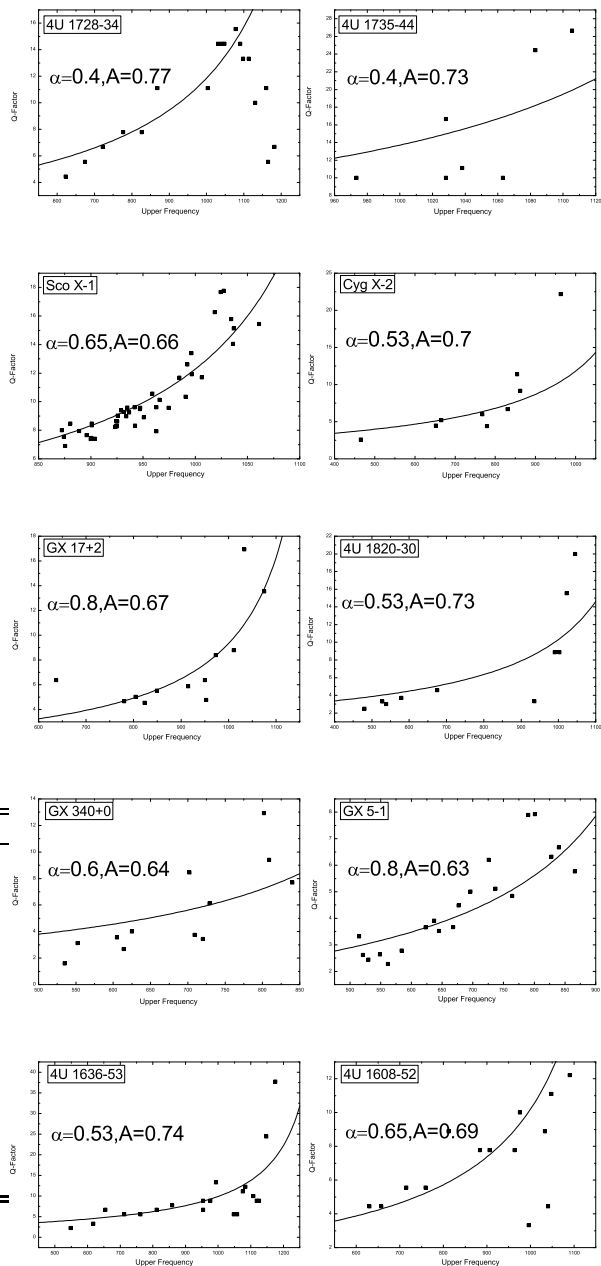


Fig. 3. The same meaning with Fig. 2 but for separated sources (five Atoll and five Z sources). The model curves are plotted with the different extent parameter α and averaged mass density parameter A that were derived from the detecting data (Zhang et al. 2007).

the radial extent of contributing to upper frequency is about 3 km.

While making comparisons of model to the Q-factors of five Atoll and five Z sources separately, as shown in Fig. 3, we notice that there exist a big discrepancy in 4U 1728-34 at high frequency, more errors in Cyg X-2 and GX 340+0. On the unusual abrupt drop of upper Q-factor of 4U 1728-34, it is ascribed as the effect of ISCO (Barret, Olive & Miller 2006). On the upper Q-factors of Cyg X-2 and GX 340+0, we argue that there might not only exist a radial extent but also a verti-

cal extent to contribute to the QPO emission regions, and if the thickness extent of transition layer is considered it might arise new ingredients on the QPO profiles. On the thickness of accretion disk and QPO phenomenon, we refer to the recent work by Chakrabarti et al. (2009). We think that the complete description of QPO profile should take both radial and thickness extents around preferred radius into account, since the pileup blob of accreting plasma interacts with magnetosphere to produce the fruitful X-rays in a spacial domain. Moreover, it is remarked that our model on the profile of kHz QPO is concentrated to the upper frequency Q_2 , which cannot be automatically applied to the lower frequency Q_1 , and in fact the observations of Q_2 and Q_1 are apparently different. We ascribe the profile width of ν_2 to the radial width of the transition layer of magnetosphere-disk, which is scaled by $\delta r = r-R$, but the profile width of ν_1 should be not related to this width. Therefore, there does not exist a relation between Q_1 and Q_2 , although a relation between the upper and lower frequencies can be clearly expressed. It is a subsequent work to figure out the mechanism for the profile of lower kHz QPO Q_1 .

4. acknowledgements

It is a pleasure to thank S.K. Chakrabarti for discussions, to M. Mendez and D. Barret for providing the QPO data. This work has been supported by the National Natural Science Foundation of China (NSFC 10773017) and the National Basic Research Program of China (2009CB824800).

References

- Abramowicz M. A., Karas V., Kluzniak W., Lee W. H., Rebusco P. 2003, PASJ, 55, 467
 Barret, D., Boutelier, M., & Miller, M. C. 2008, MNRAS, 384, 1519
 Barret D., Kluzniak W., Olive J. F., Paltani S., Skinner G. K. 2005a, MNRAS, 357, 1288
 Barret D., Olive J. F., Miller M. C. 2005b, MNRAS, 361, 855
 Barret D., Olive J. F., Miller M. C. 2005c, Astron. Nachr., 326, 808
 Barret D., Olive J. F., Miller M. C. 2006, MNRAS, 370, 1140
 Barret D., Olive J. F., & Miller M. C. 2007, MNRAS, 376, 1139
 Belloni T., Mendez M., Homan J. 2005, A&A, 437, 209
 Belloni T., Méndez M. & Homan J. 2007, MNRAS, 376, 1133
 Belloni T., Psaltis D., van der Klis M. 2002, ApJ, 572, 392
 Boutelier M., Barret D., & Miller M. C. 2009, MNRAS, 399, 1901
 Boutelier M., Barret D., Lin Y., Török G. 2010, MNRAS, 401, 1290
 Chakrabarty D., Morgan E. H., Munro M. P. et al. 2003, Nature, 424, 42
 Chakrabarti S. K., Debnath D., Pal P.S., Nandi A., Sarkar R., Samanta M. M., Wiita P.J., Ghosh H., Som D., 2009, Brief entry Published in "Berlin 2006, Marcel Grossmann Meeting on General Relativity" 569-588, arXiv:0903.1482
 Elsner R. F. & Lamb F. K. 1977, APJ, 215, 897
 Hasinger G. & van der Klis M. 1989, A&A, 225, 79
 Hasinger G. 1990, RvMA, 3, 60
Kluzniak W. 1998, ApJ, 509, 37
 Kluzniak W., Abramowicz M. A. 2001, Acta Physica Polonica B, 32, 3605
Kluzniak W., Michelson P., Wagoner R. V. 1990, ApJ, 358, 538
 Kulkarni A. K. & Romanova M. M. 2008, MNRAS, 386, 673
 Méndez M. 2006, MNRAS, 371, 1925
 Méndez M., van der Klis M. 1999, ApJ, 517, L51
 Méndez, M., & van der Klis, M. 2000, MNRAS, 318, 938
 Méndez, M., van der Klis, M., & Ford, E.C. 2001, ApJ, 561, 1016
 Miller M. C., Lamb F. K., Psaltis D. 1998, ApJ, 508, 791
Naso L., Miller J. C. 2010a, A&A, 521, 31
Naso L., Miller J. C. 2010b, arXiv:1012.3194
 Psaltis D. et al. 1998, ApJ, 501, L95
 Psaltis D. et al. 1999a, ApJ, 520, 763
 Psaltis D., Belloni T., van der Klis M. 1999b, ApJ, 520, 262
 Rastätter L. & Schindler K. 1999, APJ, 524, 361
 Regev O. & Hougerat A. A. 1988, MNRAS, 232, 81
 Romanova M. M., Kulkarni A. K. & Lovelace R. V. E. 2007 (astro-ph/0711.0418)
 Ruediger G. & Pipin V. V. 2000, A&A, 362, 756
 Stela L. & Vietri M. ApJ, 1998, 492, L59
 Stella L. & Vietri M. PRL, 1999, 82, 17
 Stella L., Vietri M., Morsink S. M. ApJ, 1999, 524, L63
 Titarchuk L., Lapidus I. & Muslimov A. 1999, APJ, 499, 315
 Titarchuk L. & Osherovich V. 1999, APJ, 518, L95
 Titarchuk L. & Wood K. 2002, APJ, 577, L23
 Török G. 2009, A&A, 497, 661
 van der Klis M. 2000, ARA&A, 38, 717
 van der Klis M. 2006, A review of rapid X-ray variability in X-ray binaries inn Compact stellar X-ray sources, W.H.G. Lewin & M. van der Klis (eds.), Cambridge University Press, p. 39; (astro-ph/0410551).
 van der Klis M. 2008, AIPC., 1068, 163
 Wijnands R., van der Klis M., Homan J. et al. 2003, Nature, 424, 44
 Wijnands R. 2005, [astro-ph/0501264]
Yu W. F., van der Klis M. 2002, ApJ, 567, 67
Yu W. F., van der Klis M., Jonker P. G. 2001, ApJ, 559, 29
 Zhang C. M. 2004, A&A, 423, 401
 Zhang C. M. 2008, AIPC., 1068, 174
 Zhang C. M., Yin H. X., Zhao Y. H., Chang H. K. & Song L. M. 2007, Astron.Nachr., 328, 475
 Zhang C. M., Yin H. X., Zhao Y. H., Zhang F. & Song L. M. 2006a, MNRAS, 366, 1373
 Zhang F., Qu J. L., Zhang C. M. et al. 2006b, ApJ, 646, 1116
 Zhang C. M., Wei Y. C., Yin H. X., Zhao Y. H., Lei Y. J., Song L. M., Zhang F., Yan Y., 2010, Sci.China, 53, 114